

Flux trapping behavior in a joint-less closed-loop 2G-HTS coil under multi-pulse magnetic field excitation

Hao Dong(董浩), Daxing Huang(黄大兴), Hao Yu(于昊), Hongwei Gu(古宏伟), and Fazhu Ding(丁发柱)
Citation: Chin. Phys. B, 2025, 34 (**7**): 070702. DOI: 10.1088/1674-1056/adcdf0
http://cpb.iphy.ac.cn; http://iopscience.iop.org/cpb

What follows is a list of articles you may be interested in

Vector magnetometry in zero bias magnetic field using nitrogen-vacancy ensembles

Chunxing Li(李春兴), Fa-Zhan Shi(石发展), Jingwei Zhou(周经纬), and Peng-Fei Wang(王鹏飞)
Chin. Phys. B, 2024, 33 (**10**): 100701. DOI: 10.1088/1674-1056/ad73af

Dynamic analysis of a novel multilink-spring mechanism for vibration isolation and energy harvesting

Jia-Heng Xie(谢佳衡), Tao Yang(杨涛), and Jie Tang(唐介)
Chin. Phys. B, 2024, 33 (**5**): 050706. DOI: 10.1088/1674-1056/ad21f6

Surface lattice resonance of circular nano-array integrated on optical fiber tips

Jian Wu(吴坚), Gao-Jie Ye(叶高杰), Xiu-Yang Pang(庞修洋), Xuefen Kan(阚雪芬), Yan Lu(陆炎), Jian Shi(史健), Qiang Yu(俞强), Cheng Yin(殷澄), and Xianping Wang(王贤平)
Chin. Phys. B, 2023, 32 (**12**): 120701. DOI: 10.1088/1674-1056/acf491

Anti-Stokes/Stokes temperature calibration and its application in laser-heating diamond anvil cells

Minmin Zhao(赵旻旻), Binbin Wu(吴彬彬), Jingyi Liu(刘静仪), and Li Lei(雷力)
Chin. Phys. B, 2023, 32 (**9**): 090704. DOI: 10.1088/1674-1056/accd55

Design of an ultrafast electron diffractometer with multiple operation modes

Chun-Long Hu(胡春龙), Zhong Wang(王众), Yi-Jie Shi(石义杰), Chang Ye(叶昶), and Wen-Xi Liang(梁文锡)
Chin. Phys. B, 2021, 30 (**9**): 090701. DOI: 10.1088/1674-1056/ac11cd

---

Flux trapping behavior in a joint-less closed-loop 2G-HTS coil under multi-pulse magnetic field excitation

Hao Dong(董浩)[1,2], Daxing Huang(黄大兴)[1,2,3,†], Hao Yu(于昊)[1,2], Hongwei Gu(古宏伟)[1,2,3,‡], and Fazhu Ding(丁发柱)[1,2,3,§]

[1] *Key Laboratory of Applied Superconductivity and Institute of Electrical Engineering, Chinese Academy of Sciences, Beijing* 100190, *China*
[2] *University of Chinese Academy of Sciences, Beijing* 100049, *China*
[3] *Shandong Key Laboratory of Advanced Electromagnetic Conversion Technology and Institute of Electrical Engineering and Advanced Electromagnetic Drive Technology, Qilu Zhongke, Jinan* 250100, *China*

(Received 23 February 2025; revised manuscript received 11 April 2025; accepted manuscript online 17 April 2025)

Second-generation high-temperature superconducting (2G-HTS) magnets operating in persistent current mode (PCM) hold great promise for applications such as magnetic resonance imaging. The development of joint-less closed-loop magnets has effectively tackled the challenges of fabricating joints for REBCO tape. However, certain closed-loop magnets cannot utilize conventional persistent current switches (PCS) and instead require multi-pulse magnetization techniques. This study explores the effects of multi-pulse magnetic field excitation on the flux trapping behavior of a four-pancake coil (FPC). A detailed comparison of the effects of different pulse types and periods on the FPC reveals that the background magnetic field exceeds the critical magnetic field of the coil, thereby creating resistance in the superconducting loop. The critical magnetic field of the FPC is determined experimentally, and a reasonable speculation on the multi-pulse field excitation mechanism is presented.

Keywords: joint-less coil, second-generation high-temperature superconducting (2G-HTS) coil, multi-pulse, excitation

PACS: 07.55.Db, 74.72.–h, 84.71.Ba, 84.71.Mn

DOI: 10.1088/1674-1056/adcdf0 **CSTR:** 32038.14.CPB.adcdf0

1. Introduction

Second-generation high-temperature superconducting (2G-HTS) magnets operating in persistent current mode are crucial for devices requiring high magnetic field stability, such as magnetic resonance imaging (MRI) and nuclear magnetic resonance (NMR) devices.[1–6] The superior critical magnetic fields and critical temperatures of 2G-HTS magnets have driven extensive research and gradual industrialization.[7–10] Due to the immaturity of joint fabrication technologies in $REBa_2Cu_3O_{7-\delta}$ (REBCO, RE: rare earth) tape, researchers have proposed various joint-less closed-loop structures to enhance magnetic field stability, which has demonstrated preliminary success.[11,12] Up to now, several joint-less designs have been explored, including 2G-HTS rings, joint-less stacked pancake (JSP) coils, and bitter-like HTS magnets.[13–16] In our previous work, we proposed a four-pancake coil structure with potential for commercial applications, referred to as the 'four-pancake coil (FPC)'.[17,18]

However, the excitation methods for joint-less closed-loop coils remain significantly constrained, posing a major challenge to their development. For instance, bitter-like HTS magnets cannot be energized using conventional persistent current switches (PCS) and often require field cooling or multi-pulse techniques.[14,19–21] In previous studies, it has been reported that successful charging of 2G-HTS closed-loop magnets has been achieved using a multi-pulse background magnetic field.[21–23] The flux trapping behavior of closed-loop coils under different pulse waveforms has been less reported.

Therefore, this paper presents a detailed investigation into the effects of multi-pulse magnetic field excitation on the flux trapping behavior of the FPC. By energizing the background magnetic field with a programmable AC power supply, a systematic comparison was made between the effects of slow-rise steep-fall pulse, steep-rise slow-fall pulse, and symmetric pulse on the flux trapping characteristics of the FPC. A possible theoretical explanation of the experimental results was provided by determining the critical magnetic field of the FPC. These findings hold significant potential for advancing the multi-pulse magnetic field excitation of joint-less coils and improving their practical applications.

2. Structure and testing

The joint-less closed-loop coil was fabricated utilizing REBCO tapes supplied by Samri Co., Ltd., China. In previous studies, the REBCO tape was precisely slit along its

†Corresponding author. E-mail: huangdaxing@mail.iee.ac.cn
‡Corresponding author. E-mail: guhw@mail.iee.ac.cn
§Corresponding author. E-mail: dingfazhu@mail.iee.ac.cn

© 2025 Chinese Physical Society and IOP Publishing Ltd. All rights, including for text and data mining, AI training, and similar technologies, are reserved.

central axis while preserving the endpoints, with each half subsequently wound into a double-pancake coil configuration. This process ultimately formed a compact four-pancake structure (referred to as the FPC) characterized by a jointless design.[17] Notably, this coil exhibits zero resistance in its closed-loop configuration, thereby offering a highly stable and reliable structure for magnetic applications.

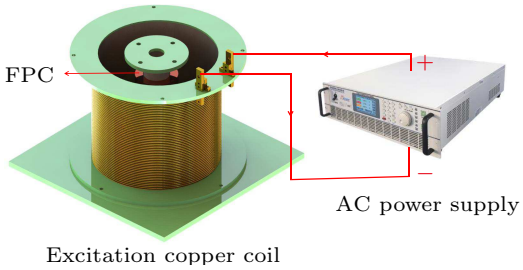


Fig. 1. Schematic diagram of the excitation experiment.

The background field coil was fabricated by helical layer-winding of enameled copper wire, and it is electrically connected via copper electrodes to an external AC power supply to generate the requisite background magnetic field. A central support frame was designed at the center of the background field coil, allowing the FPC to be mounted coaxially, as illustrated in Fig. 1. The key parameters of the copper coil, the original REBCO tape before slitting, and the final FPC configuration are systematically presented in Table 1.

Table 1. Key parameters of the copper coil, REBCO tape, and FPC.

Parameters of the copper coil	
Length	~ 550 m
Linear diameter	0.6 mm
Inside coil diameter	150 mm
Outside coil diameter	~ 160 mm
Turns	~ 1000 turns
Winding method	layer wound
REBCO tape parameters (before slitting)	
Length	5 m
Encapsulation process	silver
Width	12 mm
Critical current (77 K, Self-field)	160 A
FPC parameters	
Insulation method	no-insulation
Inside coil diameter	34 mm
Turns	~ $21 \times 2 \times 2$
Coil critical current (77 K)	~ 30 A

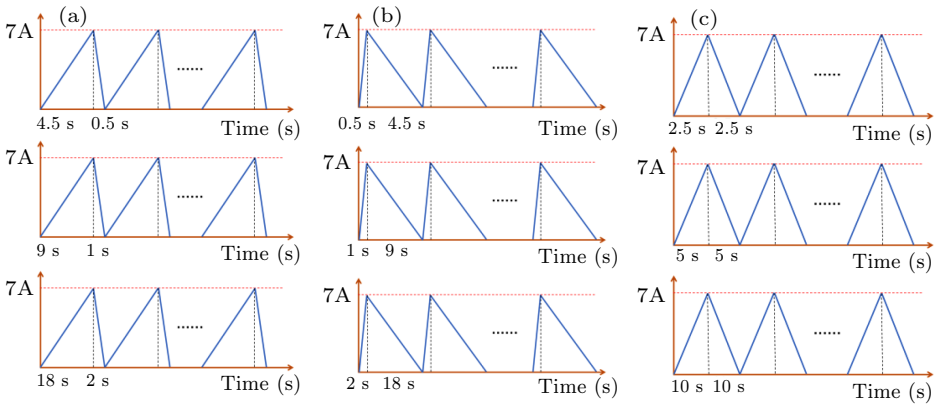


Fig. 2. The three pulse waveforms output by the AC power source.

The output pulse of the AC power source was programmatically controlled using LABVIEW software, as shown in Fig. 2. This study investigates the effects of three pulse waveforms (slow-rise steep-fall pulse, steep-rise slow-fall pulse, and symmetric pulse) on excitation under three different pulse periods. The steep-rise and steep-fall segments each constitute 10% of the total period. In the symmetric pulse, the current rises and falls at the same rate. The peak value of the excitation current was set to 7 A, at which the magnetic field generated in the copper coil is close to the critical field strength of the superconducting coil at 77 K.

The experimental setup is immersed in a liquid nitrogen environment, with the FPC sleeved onto the central cylindrical support inside the copper coil, and the Hall sensor positioned on the inner side of the central tube, as depicted in Fig. 3(a). To determine the critical magnetic field of the FPC, a PCS is used to excite the FPC, as illustrated in Fig. 3(b). The PCS comprises two thin-film heaters, which are externally connected to a DC power supply.[24–26] By selectively heating a small section of the tape (~ 1 cm), the PCS induces quenching of the wrapped tape, thereby enabling its switching functionality.

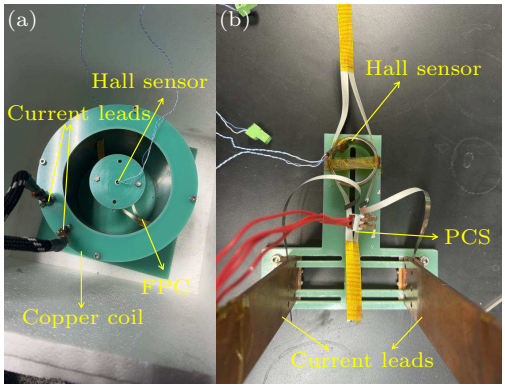


Fig. 3. (a) Multi-pulse magnetic field excitation device and (b) the FPC is excited using a persistent current switch.

3. Results and discussion

In this work, the positive and negative values of the magnetic field detected by the Hall sensor are used to indicate the direction of the trapped field. Specifically, the axial upward magnetic field is defined as a positive value, while the axial downward magnetic field is defined as a negative value. The current induced inside the FPC during the increasing phase of the pulsed magnetic field is defined as positive, whereas the current induced during the decreasing phase of the pulsed magnetic field is defined as negative. Initially, the FPC is charged using a slow-rise steep-fall pulse. According to Faraday's law of electromagnetic induction,[27] as the background field increases, a positive current is induced inside the FPC, generating a magnetic field opposite to the background field. Conversely, when the background field rapidly decreases, a negative current is induced inside the FPC. Notably, during a single pulse cycle, the magnitude of the negative current exceeds that of the positive current. Consequently, the net current (calculated as positive current minus negative current) follows the direction of the negative current, resulting in the magnetic field generated by the FPC after one cycle being in the same direction as the initial increase in the background magnetic field. Experimental results for pulse periods of 5 s, 10 s, and 20 s are presented in Fig. 4.

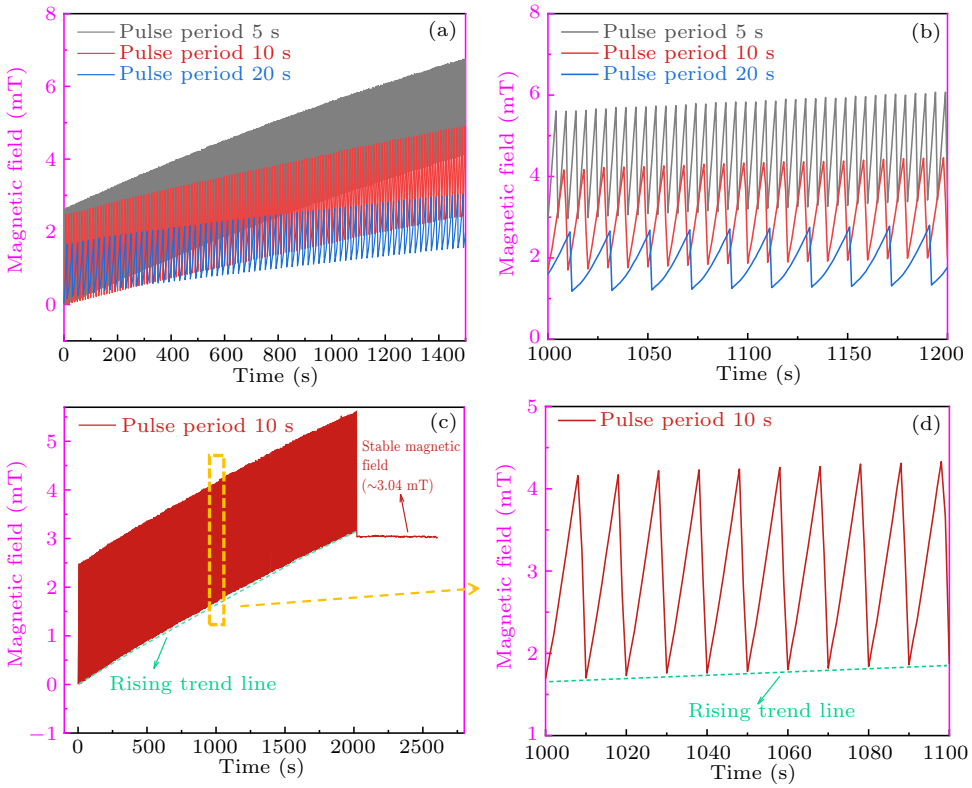


Fig. 4. Impact of the slow-rise steep-fall pulse on flux trapping in the FPC.

As shown in Fig. 4(a), the magnetic field measured by the Hall sensor gradually increases with the number of pulses, and the induced magnetic field inside the FPC aligns with the background magnetic field. A notable observation is that a shorter excitation period results in higher excitation efficiency, which is related to the number of pulses. Figure 4(b) presents a magnified view of Fig. 4(a), elucidating the impact of different excitation periods on the field increase process. The experiment with a 10-s excitation period was examined in detail, showing that the FPC's magnetic field increases along an upward trend as the number of pulses increases. The lowest magnetic field value of each pulse corresponds to the trapped field in the FPC when the background magnetic field is zero, as shown in Fig. 4(c). Experimental results demonstrate that approximately 3.04 mT of the magnetic field was successfully trapped after about 200 pulses. The minimum field value continuously rises, and its waveform resembles that of the external background field, as shown in Fig. 4(d). This phenomenon can be attributed to the counteracting effect of the induced currents within the superconducting coil which effectively mitigates external field fluctuations. As a result, the fluctuation range is smaller than that of the external magnetic field.

However, when the experiment was repeated using the steep-rise slow-fall pulse, the FPC magnetic field direction remained consistent with the background field, and no significant change in excitation efficiency was observed. According to conventional electromagnetic theory, during the rapid rise of the background field, a positive current is induced in the FPC, generating a magnetic field in the opposite direction as the background field. Conversely, during the slow decay of the background field, a negative current is induced in the FPC. Since the magnitude of the positive current exceeds that

of the negative current, the net current (positive current minus negative current) aligns with the positive current direction, resulting in the FPC generating a magnetic field in the opposite direction of the initial increase in the background field. However, the experimental results did not exhibit this expected reversal, as shown in Fig. 5(a). Furthermore, we compared the effects of different pulse periods on excitation. The results indicate that a longer pulse period leads to a lower excitation efficiency. Figure 5(b) presents a magnified view of Fig. 5(a), revealing that the magnetic field increases in a steep-rise slow-fall pattern, consistent with the background field. Specifically, we investigated the excitation effect with a 10-s pulse period, as demonstrated in Fig. 5(c). After approximately 420 pulses, the FPC trapped a magnetic field of about 5.71 mT. The entire device is removed from the liquid nitrogen and a rapid drop in the magnetic field can be observed. Figure 5(d) provides a zoomed-in view of Fig. 5(c), showing that the magnetic field exhibits a distinct steep-rise slow-fall characteristic during the increase phase.

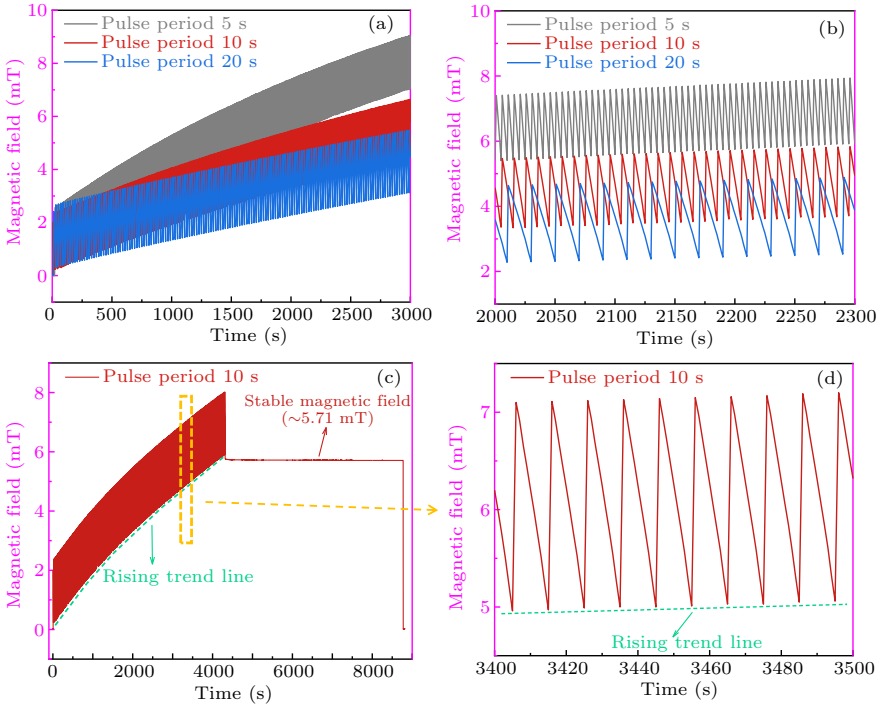


Fig. 5. Impact of the steep-rise slow-fall pulse on flux trapping in the FPC.

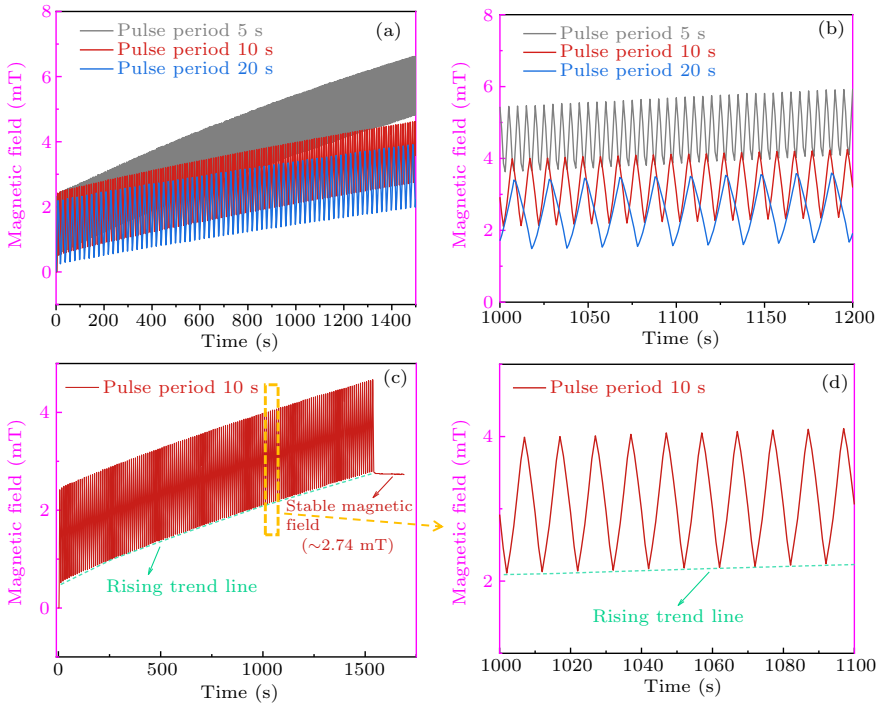


Fig. 6. Impact of the symmetric pulse on flux trapping in the FPC.

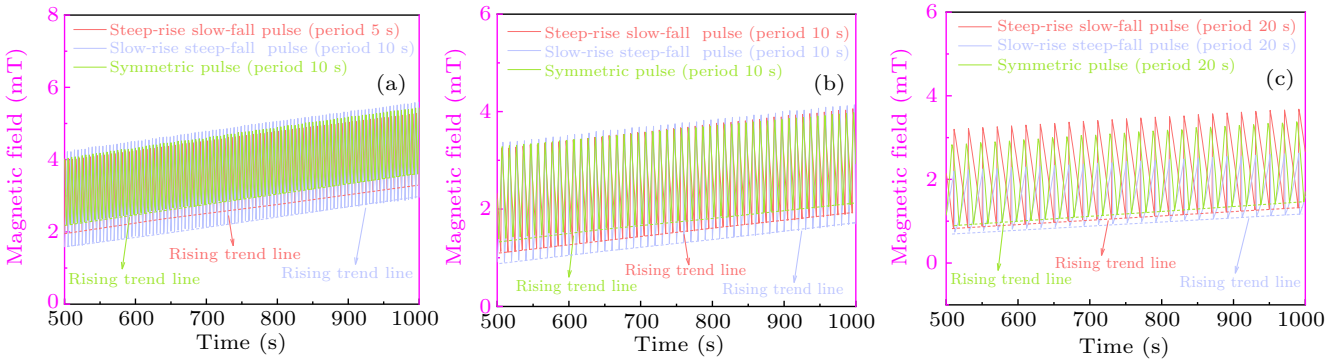


Fig. 7. Comparisons of slow-rise steep-fall pulse, steep-rise slow-fall pulse, and symmetric pulse on the magnetization process of the FPC.

Subsequently, the effect of symmetrical pulses on the trapped magnetic flux of the FPC was investigated. Symmetrical pulses were still able to generate an induced current inside the superconducting coil, as shown in Fig. 6. As the number of pulses increased, the current inside the FPC gradually increased (Fig. 6(a)). In Fig. 6(b), it can be observed that the magnetic field gradually increased after each pulse, indicating that the negative current generated within the FPC was larger than the positive current. Similarly, using a symmetric waveform with a pulse period of 10 s, the FPC successfully trapped a magnetic field of about 2.74 mT after approximately 150 pulses (Fig. 6(c)). From Fig. 6(d), it can be seen that the magnetic field exhibited asymmetry in its upward and downward amplitudes during a cycle, indicating that the positive current induced within the FPC was not symmetric in magnitude concerning the negative current.

Furthermore, the effects of the slow-rise steep-fall pulse, steep-rise slow-fall pulse, and symmetric pulse on excitation efficiency were compared. As shown in Figs. 7(a)–7(c), comparing the effect on the trapped flux of the FPC under 5-s, 10-s, and 20-s excitation periods, it can be observed that there is no too obvious difference in the excitation efficiency of different pulses in a short time. Therefore, conventional theory no longer applies in this context.

This phenomenon can be attributed to the fact that the current induced by the background magnetic field in the FPC exceeds the critical current under the magnetic field of the REBCO tape, which induces a resistance in the superconducting loop. The properties of REBCO tape can be described by the power law of the V–I properties as follows:

$$R_{\mathrm{c}} = V_{\mathrm{c}} \left(\frac{I_{\mathrm{o}}}{I_{\mathrm{c}}} \right)^{n} / I_{\mathrm{o}} = V_{\mathrm{c}} I_{\mathrm{o}}^{n-1} / I_{\mathrm{c}}^{n}, \tag{1}$$

where R_{c} represents the equivalent resistance, V_{c} is the critical criterion, I_{c} denotes the critical current, I_{o} is the operating current, and n is the n-index of the tape. According to Eq. (1), for an FPC, the strength of the background magnetic field exceeds the critical magnetic field of the coil at 77 K, resulting in $I_{\mathrm{o}} > I_{\mathrm{c}}$ and thus $R_{\mathrm{c}} \neq 0$. The presence of resistance reduces the positive current, consequently making the negative current always larger than the positive current. We consider that the asymmetry between positive and negative currents may be due to the different rates of increase of the resistance from zero to a maximum value (background magnetic field increasing phase) and decrease from a maximum value to zero (background magnetic field decreasing phase). As a result, the final current direction aligns with the negative current direction, meaning the magnetic field trapped by the FPC always corresponds to the magnetic field when the background field initially increases. To further validate this conclusion, an open-circuit experiment was conducted after removing the FPC, and the results are shown in Fig. 8. When the excitation current was set to 7 A, the induced magnetic field measured at the center Hall sensor was approximately 52 mT, which may exceed the critical magnetic field of the FPC, that is, the induced current in the FPC may exceed the critical current of the REBCO tape.

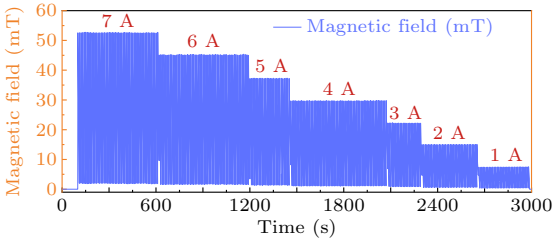


Fig. 8. Magnetic field characteristics of the background field without the FPC.

To determine the critical magnetic field of the coil, the FPC was excited using an external DC power supply and PCS, and the critical magnetic field of the FPC at 77 K was obtained using the field decay method. The field-decay rate of the coil can be described by

$$B_{\mathrm{t}} = B_0 \, \mathrm{e}^{-R_{\mathrm{c}} t / L}, \tag{2}$$

where B_{t} is the induced magnetic field, B_0 is the initial induced magnetic field, t is the time variable, and L is the self-inductance of the coil. The critical field was approximately 50 mT, as shown in Fig. 9. When the background magnetic field exceeds the critical field of the FPC, the presence of loop

resistance causes the magnetic field to gradually decay. The stable value of the decayed magnetic field can then be used to determine the critical magnetic field of the coil. Based on this experimental result, we consider that the current inside the FPC only gradually accumulates when the background field exceeds the critical field strength of the coil. Tests with smaller pulse current amplitudes (5 A) showed that no significant increase in magnetic field was observed in the FPC, regardless of the number of pulses.

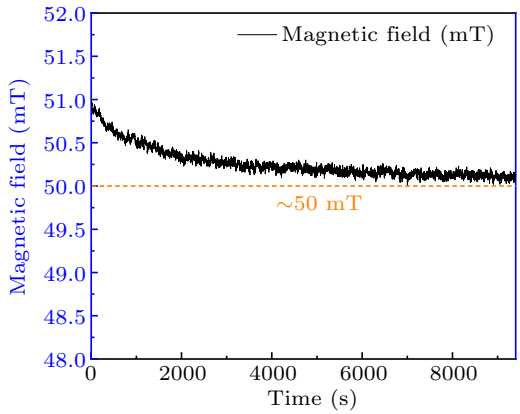


Fig. 9. The critical magnetic field of the FPC at 77 K, measured through the magnetic field decay method.

4. Conclusion and perspectives

This study investigates the effects of multi-pulse magnetic field excitation on the flux trapping behavior of an FPC. Furthermore, the excitation efficiency when using three different types of pulses for excitation is mainly related to the pulse period and less correlated to the pulse shape. Based on the experimental results, it can be further speculated that when the background field strength exceeds the critical field strength of the FPC, a resistance is generated within the superconducting loop, resulting in a smaller induced positive current. As a result, the negative current is always larger than the positive current, and the final current direction aligns with the negative current direction, leading to the trapped field in the FPC aligning with the background field.

The critical magnetic field of the FPC was determined to be about 50 mT using the magnetic field decay method, indicating that the net current inside the superconducting coil gradually accumulates when the background magnetic field exceeds the critical magnetic field of the FPC under the multi-pulse magnetic field. This study provides theoretical and experimental support for the flux trapping behavior of joint-less closed-loop superconducting coils under multi-pulse magnetic field excitation.

Acknowledgements

Project supported by the National Key Research and Development Program of China (Grant No. 2022YFE03150203), the National Natural Science Foundation of China (Grant Nos. U2032217, 52072366, and 52477031), and Shandong Provincial Natural Science Foundation (Grant No. ZR2024ME217).

References

[1] Hazelton D W, Rice J A, Hascicek Y S, Weijers H W and Vansciver S W 1995 *IEEE Trans. Appl. Supercond.* **5** 234
[2] Kim W S, Lee S, Kim Y, Lee J Y, Park S H, Lee J K, Hong G W, Han J and Choi K 2015 *IEEE Trans. Appl. Supercond.* **25** 4301504
[3] Parkinson B 2017 *Supercond. Sci. Technol.* **30** 014009
[4] Wang Y, Wang Q, Wang H, Chen S, Hu X, Liu Y and Liu F 2022 *Supercond. Sci. Technol.* **35** 014001
[5] Lee H G, Kim J G, Lee S W, Kim W S, Lee S W, Choi K D, Hong G W and Ko T K 2006 *Physica C* **445** 1099
[6] Li Z and Zheng G Q 2018 *Chin. Phys. B* **27** 077404
[7] Yoon S, Kim J, Cheon K, Lee H, Hahn S and Moon S H 2016 *Supercond. Sci. Technol.* **29** 04lt04
[8] Kim K, Bhattarai K R, Jang J Y, Hwang Y J, Kim K, Yoon S, Lee S and Hahn S 2017 *Supercond. Sci. Technol.* **30** 065008
[9] Bai H, Bird M D, Cooley L D, Dixon I R, Kim K L, Larbalestier D C, Marshall W S, Trociewitz U P, Weijers H W, Abraimov D V and Boebinger G S 2020 *IEEE Trans. Appl. Supercond.* **30** 4300405
[10] Liu S, Wang L, Chen Y, Wang L, Zhou B, Hu X, Cheng J and Wang Q 2023 *Supercond. Sci. Technol.* **36** 064002
[11] Kulikov I V, Chernykh M Y, Krylova T S, Yashkin D S, Chernykh I A and Zanaveskin M L 2020 *Supercond. Sci. Technol.* **33** 015001
[12] Huang D, Shang H, Xie B, Zou Q, Dong H, Wang K, Zhang L, Gu H and Ding F 2022 *Supercond. Sci. Technol.* **35** 075004
[13] Sheng J, Zhang M, Wang Y, Li X, Patel J and Yuan W 2017 *Supercond. Sci. Technol.* **30** 094002
[14] Hu Y, Wang Y, Yuan X, Chen H, Liu M, Wang M, Peng C and Pi W 2019 *IEEE Trans. Appl. Supercond.* **29** 4900505
[15] Brialmont S, Dular J, Wera L, Fagnard J F, Vanderheyden B, Geuzaine C, Hahn S, Patel A and Vanderbemden P 2023 *Supercond. Sci. Technol.* **36** 054004
[16] Hou Y B, Wang Y S, Kan C T, Yuan X and Pi W 2018 *Chin. Phys. Lett.* **35** 067402
[17] Dong H, Huang D, Wang T, Gu H and Ding F 2024 *Supercond. Sci. Technol.* **37** 015003
[18] Dong H, Huang D, Yu H, Gu H and Ding F 2024 *Superconductivity* **12** 100139
[19] Taylor R W, Weijers H W, Ainslie M D, Congreve J V J, Durrell J H, Badcock R A and Bumby C W 2024 *Supercond. Sci. Technol.* **37** 03lt01
[20] Yuan X, Wang Y, Hou Y, Kan C, Cai C and Sun M 2018 *IEEE Trans. Appl. Supercond.* **28** 4603005
[21] Hu Y, Wang Y, Lu Y, Chen H, Liu M, Yuan X, Wang M and Pi W 2019 *IEEE Trans. Appl. Supercond.* **29** 6801905
[22] Yuan X, Wang Y, Qiao Y, Wang Y and Kang Q 2021 *IEEE Trans. Appl. Supercond.* **31** 4602505
[23] Wang J W, Wang Y S, Chai H, Zhu L F and Pi W 2022 *Chin. Phys. B* **31** 037402
[24] Tosaka T, Kuriyama T, Yamaji M, Kuwano K, Igarashi M and Terai M 2004 *IEEE Trans. Appl. Supercond.* **14** 1218
[25] Li C, Geng J, Gawith J, Shen B, Zhang X, Zhang H, Ma J and Coombs T A 2018 *IEEE Trans. Appl. Supercond.* **28** 4603205
[26] Li C, Geng J, Shen B, Li X, Gawith J, Ma J, Yang J and Coombs T A 2019 *IEEE Trans. Appl. Supercond.* **29** 4900704
[27] Redzic D V 2018 *Eur. J. Phys.* **39** 025205